Front. Optoelectron. 2012, 5(2): 157–170
DOI 10.1007/s12200-012-0237-2

REVIEW ARTICLE

Vertical-external-cavity surface-emitting lasers and quantum dot lasers

Guangcun SHAN (✉)[1,2], Xinghai ZHAO[1,3], Mingjun HU[2], Chan-Hung SHEK[2], Wei HUANG[4]

1 State Key Laboratory of Functional Materials for Informatics, Chinese Academy of Sciences, Shanghai 200050, China
2 Department of Physics and Materials Science, City University of Hong Kong, Hong Kong, China
3 Institute of Electronic Engineering, China Academy of Engineering Physics, Mianyang 621900, China
4 Institute of Advanced Materials, Nanjing University of Posts and Telecommunications, Nanjing 210046, China

Abstract The use of cavity to manipulate photon emission of quantum dots (QDs) has been opening unprecedented opportunities for realizing quantum functional nanophotonic devices and quantum information devices. In particular, in the field of semiconductor lasers, QDs were introduced as a superior alternative to quantum wells (QWs) to suppress the temperature dependence of the threshold current in vertical-external-cavity surface-emitting lasers (VECSELs). In this work, a review of properties and development of semiconductor VECSEL devices and QD laser devices is given. Based on the features of VECSEL devices, the main emphasis is put on the recent development of technological approach on semiconductor QD VECSELs. Then, from the viewpoint of both single QD nanolaser and cavity quantum electrodynamics (QED), a single-QD-cavity system resulting from the strong coupling of QD cavity is presented. In this review, we will cover both fundamental aspects and technological approaches of QD VECSEL devices. Lastly, the presented review here has provided deep insight into useful guideline for the development of QD VECSEL technology, future quantum functional nanophotonic devices and monolithic photonic integrated circuits (MPhICs).

Keywords vertical-external-cavity surface-emitting lasers (VECSELs), quantum dot (QD), QD laser, quantum electrodynamics (QED), cavity QED

1 Introduction

Semiconductor quantum dots (QDs) have attracted a lot of interest for both their fundamental physics and potential applications ranging from optoelectronics to quantum information processing [1–9]. Epitaxially grown semiconductor QDs by Stranski-Krastanov self-organized method using molecular beam epitaxy (MBE) or metalorganic vapor phase epitaxy (MOVPE) have demonstrated their potential as ultrafast semiconductor lasers [5,6] and semiconductor optical amplifiers (SOAs) [7] for optical communication systems, showing new functionalities and excellent performances. Notably, a different approach for the fabrication of QDs is based on wet chemistry for synthesizing of colloidal QDs [8], and a facile microwave-assisted synthesis of core-shell NCs in aqueous solution has been further developed in 2006, which opens up a promising avenue for synthesizing NCs with high fluorescence efficiency [9]. Typical colloidal QDs are nanometer-sized core-shell structures, and the role of the shell is to engineer the band structure of the QDs and to passivate the core surface to reduce surface defects and improve their efficiency and photostability [9,10].

On the other hand, semiconductor lasers are used in a wide range of important applications, such as optical fiber communication, digital optical recording, laser materials processing, biology and medicine, imaging, spectroscopy, and some others. In particular, the vertical-external-cavity surface-emitting lasers (VECSELs) developed in the mid-1990s [11] to overcome problems with conventional semiconductor lasers, have gained reputation as a superior technology for optical communication system applications. This success was mainly due to the VECSEL's lower integration manufacturing costs and higher reliability compared to semiconductor edge-emitting lasers. Moreover, in recent years, it has been seen an increasing use of semiconductor QDs as gain component of different VECSEL devices of design [6,12,13]. In this review, we discuss the properties and development of QD VECSEL devices. Based on the features of QD lasers, the

Received December 29, 2011; accepted February 9, 2012

E-mail: guangcunshan@mail.sim.ac.cn

experimental progresses on semiconductor QD VECSELs are reviewed in detail. Besides, from the viewpoint of both single QD nanolaser and cavity quantum electrodynamics (QED), a review of a single-QD-cavity system is also presented.

2 VECSELs

The versatile semiconductor diode lasers are very widely used due to their numerous advantageous properties, such as compact size, scalability, lower integration manufacturing costs, electrical current laser excitation and modulation and excellent reliability. In this section, we focus on the basic structure, properties and advantages of semiconductor VECSELs in comparison to conventional edge-emitting lasers.

There exist two major configurations for the conventional semiconductor lasers, including edge-emitting lasers [5,14] and surface-emitting lasers [6,11–13,15] (Fig. 1). The edge-emitting lasers depicted in Fig. 1(a) use a waveguide to confine light to the plane of semiconductor chip and emit elliptical light beam from the edge of the chip, the cross section of which is typically about one by several microns. The required small waveguide dimensions for single-transverse mode operation result in the asymmetric and strong angular divergence of the laser beam. The output power of edge-emitting lasers is typically limited by the required excess heat dissipation from active region or catastrophic optical damage at semiconductor surface [16]. Up to several hundred milliwatts of output power is achievable in a single-transverse mode waveguide configuration [15,16]. For still wider waveguides, of the order of a 100 mm, single-stripe edge-emitting lasers can emit tens of watts of output power, but the waveguide is then highly multimoded in the plane of the chip, and output beam is very elongated with a very large, 80∶1, aspect ratio. Multiple stripe semiconductor laser bars can emit hundreds of watts, but with a highly multimoded output beam [16].

In contrast, surface-emitting lasers [11–13,15] with laser cavity axis emit circular fundamental transverse mode light beam with powers of several milliwatts and beam diameter of several microns perpendicular to the plane of the semiconductor laser chip shown in Fig. 1(b). In particular, the output beam with circular cross section and larger beam size of VECSELs, also known as semiconductor disk lasers, has much smaller divergence than for edge-emitting lasers. Also, the required heat dissipation limits the output power and the scaling to higher powers demands larger active areas. Furthermore, semiconductor VECSELs have emerged as low cost of fabrication, high power and high beam-quality alternative to solid-state lasers. A typical path to implement high output power laser is to use arrays of VECSELs [6,12,13,16]. For much higher powers, both laser types emit highly transverse multimoded output beams.

However, high power and good beam quality cannot be achieved simultaneously with conventional semiconductor edge-emitting or surface-emitting lasers, though it is very important for many scientific and commercial laser applications. Notably, such combination is required, such as, for efficient nonlinear optical second harmonic generation [12]. It is therefore useful and important to develop a laser that exhibits simultaneously the application required and desired laser properties, such as emission wavelength, compact size, good laser beam quality, the capability of scaling up optical power to watt and higher levels with circular output beams. It is well-known that good beam quality with fundamental transverse mode operation requires strong transverse mode control of the laser cavity [11,15]. Consequently, the VECSELs have been well developed, in which strong transverse mode control can be provided by optical cavity elements external to the laser chip, which assure that fundamental transverse mode of the laser cavity, the desired operating laser mode, has diameter approximately equal to the gain region diameter. Basic structure of VECSEL devices is depicted in Fig. 2(a) to illustrate the functions of various layers. In a VECSEL device, a thin active semiconductor chip as the key element with typical diameters range between 50 and 500 μm, containing both a gain region and multilayer high-reflectivity mirrors, is placed on a heat sink and is excited by an incident optical pump beam. Laser cavity consists of the on chip mirror and an external spherical mirror, which defines the laser transverse mode and also serves as the output coupler. For optically pumped operation, incident pump photons with higher photon energy are absorbed in

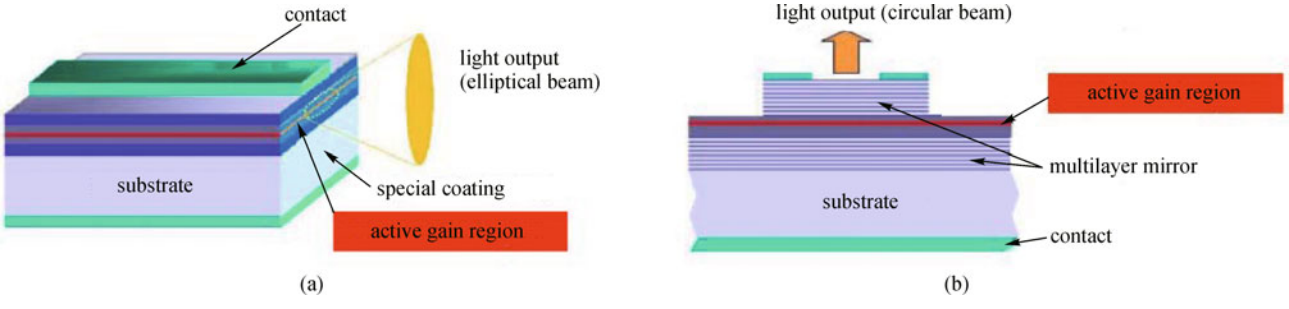

Fig. 1 Schematic structure of semiconductor edge-emitting laser (a) and surface-emitting laser (b)

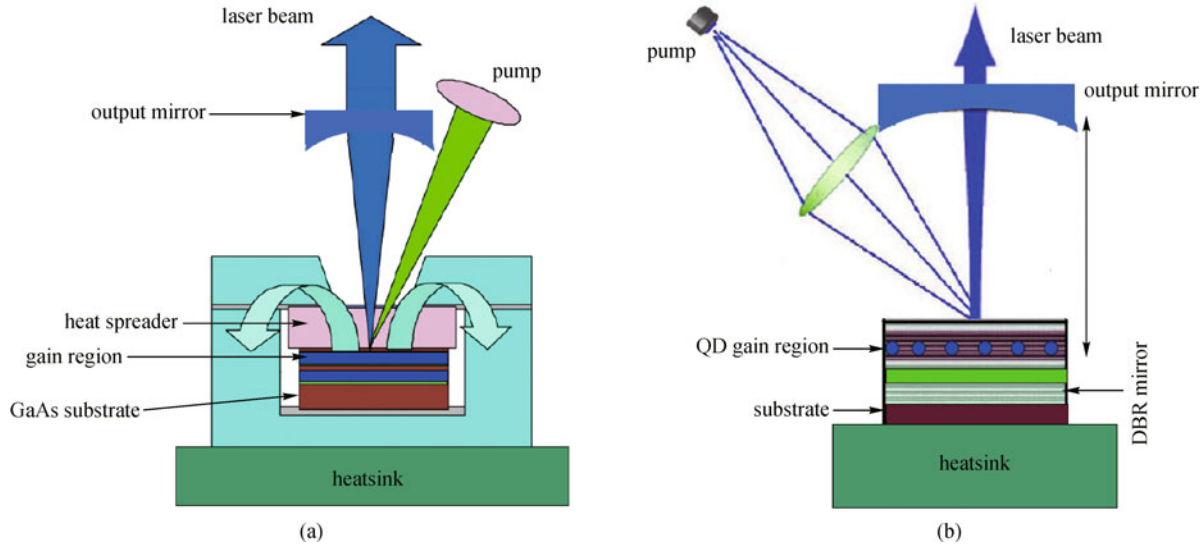

Fig. 2 Schematic structure configration of VECSEL device (a) and QD VECSEL device (b)

separate pump-absorbing layers, which also serve as the quantum well (QW) barriers, to generate electrons and holes. The excited carriers then diffuse to the smaller bandgap QWs or QD gain layers that provide gain to optical wave, emitting lasing photons with lower photon energy. These separate pump absorption and QW or QD lasing emission gain layers facilitate independent optimization of the pump absorption and laser gain properties. Typically, gain layer region thickness covers several periods of this laser mode standing wave. The pump–laser photon energy difference between the incident pump photons and the emitted laser photons, due to quantum defect, together with contributions from other lasing inefficiencies, has to be dissipated as heat from the device active region. Heat dissipation from the VECSEL active semiconductor chip is provided by heat spreaders connected to heat sinks: either a soldered heat spreader below the mirror structure or a transparent heat spreader above the surface window of the chip, or possibly both. It should be pointed out that the issues of good heat dissipation and heat sinking are critical for high-power operation of all semiconductor lasers. Without these, temperature of the active region would rise and excited carriers would escape thermally from the QWs or QDs gain layer into the barrier region, thus depleting laser gain and turning the laser off in a thermal rollover process. Such a thermal dominant rollover mechanism typically limits the output power of VECSEL devices [17]. Fortunately, the configuration of VECSELs implements good heat sinking by placement of the transparent intracavity heat spreaders in direct contact with the laser gain region without thermally resistive laser mirrors in the path of heat dissipation [15,16,18], and have the inherent potential of producing very high powers by processing large two-dimensional (2D) arrays.

Basic configuration of VECSEL lasers enables their many key advantageous properties, which can be summarized in the following aspects:

(1) Wide wavelength coverage, wavelength stability and less temperature sensitivity of wavelength: Using numerous compound semiconductor materials for different material compositions with different bandgap energies enables different lasing emission wavelengths. The use of dimensionally, or quantum-confined semiconductor active regions [6,18] allows further control of the VECSEL emission wavelengths. By adjusting the thickness of QWs or diameter of quantum wires and QDs, as well as the composition of confining barrier layers, the quantum-confined electron and hole energy levels are shifted and VECSEL acquires the additional fine control of laser emission wavelength. Moreover, the lasing wavelength in a VECSEL is very stable. Note that the emission wavelength in VECSELs is about 5 times less sensitive to temperature variations than that in edge-emitting lasers. The reason is that in VECSELs, the lasing wavelength is defined by the optical thickness of single longitudinal-mode-cavity and that the temperature dependence of this optical thickness is minimal (the refractive index and physical thickness of the cavity have weak dependence on temperature). On the other hand, the lasing wavelength in edge-emitting lasers is defined by the peak-gain wavelength, which has much stronger dependence on temperature. As a consequence, spectral linewidth for high-power arrays (where heating and temperature gradients can be significant) is much narrower in VECSEL arrays than that in edge-emitting-laser arrays (bar-stacks). Note that, over a 20°C change in temperature, the achieved emission wavelength in a QD VECSEL thus far can vary by less than 1.4 nm (compared to about 7 nm for edge-emitting lasers) due to the quantum effect of QDs, which we will discussed in detail later.

(2) Beam quality: VECSELs operate with a circular beam, fundamental transverse TEM00 mode, and essentially diffraction-limited low beam divergence. Several factors contribute to the beam quality in VECSELs. Most important, VECSEL device external-cavity optics defines and stabilizes the circular fundamental laser transverse mode; such optical elements and their stabilization effect are not available with more conventional edge and surface-emitting semiconductor lasers. If the pump spot is too large, higher order transverse laser modes with a larger transverse extent will be excited, causing multimode laser operation and thus degraded beam quality. Optimally adjusted pump spot size gives preferentially higher gain to the fundamental laser mode, while giving excess loss from the unpumped regions to the spatially wider higher order transverse modes; this stabilizes the fundamental transverse mode operation. Using pump and laser cavity optics, VECSELs have independent control allowing matching of the pump spot size and the laser fundamental transverse mode size. Large VECSEL laser beam and pump spot sizes on the chip, tens to hundreds of microns, as compared with just a few microns for edge-emitting semiconductor lasers, contribute to the mechanical stability of the VECSEL cavity, and thus also to the stability of its fundamental transverse mode operation [6]. Through proper cavity design VECSELs can emit in a circular single transverse mode beam (circular Gaussian). This simple beam structure greatly reduces the complexity and cost of coupling/beam-shaping optics (compared with edge-emitting lasers) and increases the coupling efficiency to the fiber or pumped medium. This has been a key advantage for the VECSEL devices in low-power laser applications. Another important factor affecting spatial beam quality and stability of VECSEL devices is negligible thermal lensing in the thin VECSEL semiconductor chip [6,19], when proper heat spreading/heat sinking is used. Thermal lensing and other beam phase profile distortions are caused by thermally induced refractive index gradients in the laser gain material. In VECSELs, thin semiconductor active region with good heat sinking implies that optical path length thermal distortions and hence beam profile changes and distortions are negligible. As a result, semiconductor VECSELs operate efficiently and with excellent beam quality across a wide range of operating power regimes from near to high above threshold.

(3) Higher power per unit area: VECSELs are delivering about 1350 W/cm^2 now and can deliver 2–4 kW/cm^2 in near future, while edge-emitting lasers deliver a maximum of about 500 W/cm^2 because of gap between bar to bar which has to be maintained for coolant flow.

(4) Scalability, heat-sinking, and packaging: Many optically pumped VECSEL devices have been reported with power levels between 10 mW and 60 W, a range of almost four orders of magnitude, while maintaining good beam quality. Such efficient power scalability is enabled by the laser mode and pump spot-size scalability on the semiconductor VECSEL chip. Since output power of semiconductor lasers is typically limited by heat dissipation and optical intensity-induced damage, increasing beam diameter in a VECSEL helps on both accounts, distributing heat and optical power over larger beam area. For well-designed heat sinking with thin semiconductor chips, heat flow from the laser active region into heat sink is essentially one-dimensional (1D). Therefore, increasing beam area is essentially equivalent to operating multiple lasing elements in parallel, without changing thermal or optical intensity regime of the individual lasing elements. In this scenario, both output laser power and pump power scale linearly with the active area. For high-power applications, a key advantage of VECSELs is that they can be directly processed into monolithic 2D arrays, whereas this is not possible for edge-emitting lasers. In addition, a complex and thermally inefficient mounting scheme is required to mount edge-emitter laser bars in stacks. Good heat-sinking and packaging of VECSELs have two key advantages. Due to the simple processing and heat-sinking technology it is much easier to package 2D VECSEL arrays than an equivalent edge-emitting laser bar-stack. Mounting of large high-power VECSEL 2D arrays in a "junction-down" configuration is straightforward, making the heat-removal process very efficient. In fact, VECSEL manufacturing follows the standard, well-established IC silicon industry processing.

(5) High temperature operation: VCSEL devices can be operated without refrigeration because they can be operated at temperatures to 80°C, The cooling system becomes very small, rugged and portable with this approach.

(6) Functional versatility through intracavity optical elements: Although the external optical cavity, which controls the laser transverse modes, would make these lasers more complex and requiring assembly and alignment as compared with the simple integrated surface-emitting lasers, such an external cavity of VECSELs gives tremendous versatility to VECSEL device configurations and functions. Flexible design and construction of VECSEL device cavities [20–24], such as linear two-mirror cavity, three-mirror V-shaped cavity, and four-mirror Z-shaped cavity, allow flexible insertion of intracavity optical elements. Such intracavity functional elements are very difficult to use with integrated semiconductor devices. One important option enabled by the external cavity is the insertion of intracavity spectral filters, such as Brewster's angle birefringent filters [25,26], volume gratings [27], or high-reflectivity gratings [28], to control longitudinal spectral modes of the laser and possibly to select a single longitudinal lasing mode. Moreover, the insertion of intracavity saturable absorber elements to external cavity enables VECSEL to achieve laser passive mode locking with picosecond and sub-picosecond pulse generation. In this case, the length of the external short cavity allows control of the pulse repetition

rates, with rates as high as 50 GHz [29,30]. External cavity optics also allows different beam spot sizes on the gain and absorber elements required to achieve mode locking, which controls optical intensity of the beam spots [20,31]. The open cavity of VECSELs implements placement of transparent intracavity heat spreaders in direct contact with the laser gain element without thermally resistive laser mirrors in the path of heat dissipation [24,32,33]. Since thermal management is critical for high-power VECSEL operation, the utilization of such heat spreaders tremendously broadens laser design options with chip gain, mirror, and substrate materials that do not allow effective heat removal through the on-chip mirror. Another option for VECSELs allowed by the external cavity is the microchip laser regime [6,34,35]. Low intracavity loss of VECSELs, combined with their wide gain bandwidth, allows insertion of intracavity absorption cells, such as gas cells, for intracavity laser absorption spectroscopy (ICLAS) performing sensitive measurements of extremely weak absorption lines [36]. Besides, availability of such high intracavity power, together with high beam quality, allows very efficient nonlinear optical operation, such as second harmonic generation, by inserting nonlinear optical crystals inside the external laser cavity [19,24,26]. Using intracavity second harmonic generation, VECSELs have provided efficient laser output at wavelengths not accessible by other laser materials and techniques.

To summarize, these combination advantageous properties of semiconductor VECSEL devices with excellent beam quality operate efficiently across a wide range of operating power regimes from milliwatts to tens of watts with single or multiple semiconductor gain chips resulting in versatile laser applications. In their early stage application, VECSEL devices were developed as high-power single-mode fiber-coupled sources at 980 nm for pumping Er-doped fiber and glass-waveguide amplifiers for optical fiber telecommunications systems [6]. Commercial 850 nm GaAs VCSELs have been well established for these short-reach applications. Gigabit Ethernet and Fiber Channel are currently major markets for VECSELs [6,13]. Long wavelength QD VECSELs emitting at 1.2–1.33 μm are currently attracting much interest for use in single-mode fiber metropolitan area and wide-area networks. Further optimization of the quantum defect and electron confinement energy is required for room temperature operation of high-performance QD VECSEL devices, the structure of which is depicted in Fig. 2(b). Note that in practical application there is some trade-off between output power and beam quality in VECSELs: a multimode laser beam can better overlap the pump spot and thus produce somewhat higher output power [13,16,37].

3 QD laser

The approach of quantum effects aimed at modifying the electronic density of states in active layers of a heterostructure semiconductor laser to achieve a spectral tuning ability without changing chemical composition [38,39]. In this section, we focus on the basic properties and development of semiconductor QD lasers.

As shown in Fig. 3, the quantum effect increases with the progressive reduction in dimensionality: from the square root dependence of a bulk solid, through a step-like dependence of QWs and an inverse square root dependence of quantum wires to the discrete delta function of QDs. As a result, nonequilibrium charge carriers injected into a size-quantized semiconductor gradually concentrate on the band edges. Note that, in bulk material charge carriers are redistributed within the continuous distribution function to higher energy states as the temperature is increased. These carriers do not contribute to the inversion at lasing energy, and thus additional injection current is required to maintain a constant inversion condition. The effect of QD optical gain was analyzed for laser structures

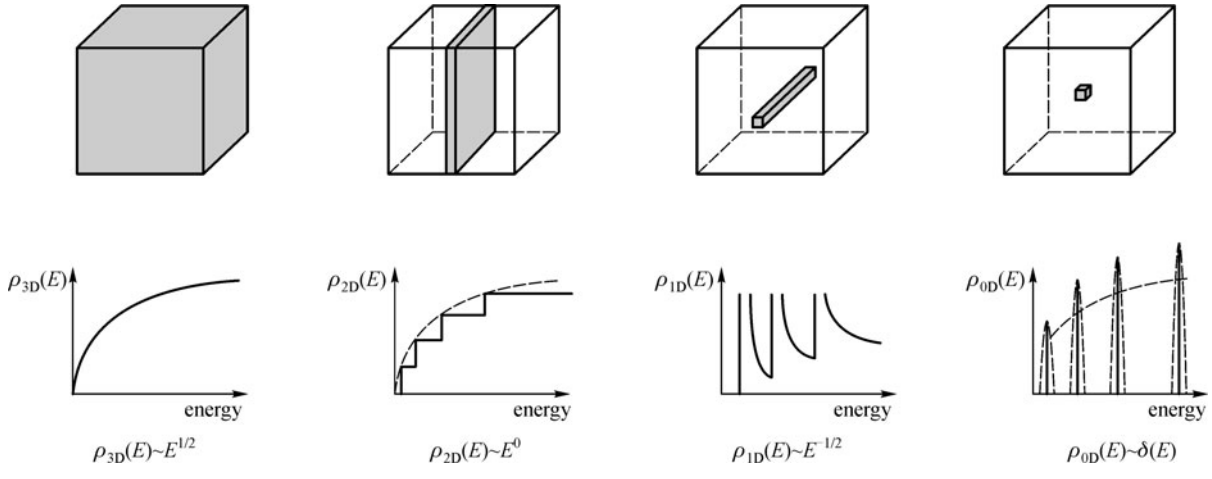

Fig. 3 Schematic illustration of quantum effects (density of states) from bulk, QW, quantum wire to QD

based on InP and GaAs QD materials [40–43]. Theoretical modeling work assumed a single active layer of QDs, a cubic shape of uniform size in the QD ensemble, and hence an equal localization of carriers in the QDs. The relationship for active GaAs layers embedded in $Al_{0.2}Ga_{0.8}$ As shows a clear increase in the maximum gain as the dimensionality is reduced. The increase in maximum gain is also reflected in a decrease in the lasing threshold current density J_{th}. The lasing threshold is generally reached, if the modal gain g_{mod} just equilibrates the internal losses α_{int} and those of the cavity mirrors α_{mirr},

$$g_{mod} = a_{int} + a_{mirr}. \quad (1)$$

Notably, QDs are nanosized semiconductors in the range of the de Broglie wavelength of charge carriers in all spatial directions, leading to atom-like, fully quantized states of confined electrons and holes. The discrete nature of the energy states causes the unique properties of QDs, not observed with higher dimensionality systems. Although the optical confinement factor of a QD layer is significantly smaller than that of a QW, the material gain of QD media g_{mat} exceeds that of QWs by far [6,38], because of the increase in the density of states described above, as well as an increased overlap of confined electron and hole wave functions and thereby an increase in the exciton binding energy due to quantum confinement. The oscillator strength of radiative recombination is thereby significantly enhanced. Device applications of carrier confinement of QD media in all three dimensions promised significant advantages over the 1D confinement of QWs [39,40]. Since the number of states in a QD layer is small compared to those of a QW, a low lasing threshold and a low gain saturation level are easily reached in single active layers for QD lasers. In order to increase both confinement factor and gain saturation level, actual QD lasers generally comprise a stack of QD layers. As a result of confinement factor and material gain, a largely comparable modal gain is found in QD lasers. Moreover, the behavior of decrease in the temperature sensitivity of the threshold current density can be expected and observed due to the reduction in dimensionality, leading in the ultimate limit of a zero-dimensional (0D) nanostructure to a lasing threshold current density J_{th} being independent of temperature. From the viewpoint of low-dimensional condensed matter physics, low temperature sensitivity of 0D nanostructures is a direct consequence of the modified electronic density of states [38,39]. As shown in Fig. 3, the occupation in a QD is described by a delta function. The charge carriers cannot be redistributed if excited states lie sufficiently above the ground state. Besides, it is worthwhile to emphasize that quantum size effects of QDs leading to an increase in the density of states near the band edges can lower the lasing threshold [38]. Therefore, an ultimate microscopic limit of thresholdless semiconductor lasers is QD laser. Besides, a QD laser is expected to work under the thresholdless operation only if the exciton resonance wavelength is the same as that of the resonant wavelength of the nanocavity, and when the position is located where the electric field of the optical cavity is strongest.

As a matter of fact, research work on low dimensional nanostructures as gain media for semiconductor lasers first focused on QWs due to lacking reliable methods for fabricating sufficiently high-quality QDs at that time [6,31,36]. However semiconductor QW lasers suffer from limitations such as relatively high threshold powers, multimode operation, problems with direct modulation above 20 GHz, and difficulty in growing their distributed Bragg reflectors (DBR) for long-haul communications wavelengths. Moreover, the discrete nature of the energy states or electronic density of states causes the emergence of unique properties of QDs, which cannot be observed in higher dimensionality nanostructures [39]. As a consequence, the threshold of QD lasers is ultimately minimized (the so-called thresholdless laser) by eliminating spontaneous emission as much as possible [39,40]. Early attempts to implement the QDs by dry etching of QW structures into a laser resulted in devices with poor performance [31]. In the 1990s, the efficient approach of self-organized Stranski–Krastanow growth was applied to realize ensembles of QDs with a high areal density [40]. Since then, much work was devoted to exploit the ability of high quality Stranski– Krastanow QDs to emit at wavelength from 650 nm to 2.8 μm [44–70]. It should be noted that the radiative recombination was strongly limited due to the relaxation of captured carriers hampered by a phonon bottleneck effect, and the orthogonality of electron and hole wave functions. Besides, the inhomogeneous broadening within a QD ensemble and the assumed small total number of QDs participating in lasing operation were considered to be a major drawback to achieve sufficient output power [43,54,55]. The first injection lasers based on self-organized QDs grown using MBE were edge-emitting ridge-waveguide devices with a single layer of $In_{0.5}Ga_{0.5}As$/GaAs Stranski–Krastanow QDs [56]. The devices demonstrated the predicted advantages [41,43,54–56] of 0D nanostructures over those of higher dimensionality. A low threshold current density of 120 $A \cdot cm^{-2}$ with a low temperature sensitivity expressed by a high characteristic temperature of 350 K was observed at low temperature operation. However, the excellent performance was maintained only up to 120 K as a result of several processes, such as thermal redistribution of carriers to nonlasing states within the QDs, thermally induced escape of carriers out of the QDs, and Auger nonradiative mechanisms [57]. Later, various approaches were employed to achieve improvements of laser characteristics by MOVPE. The first MOVPE-grown QD lasers used either an InAs QD stack [58] or an $In_{0.5}Ga_{0.5}As$ QD stack [59]. Both approaches achieved ground-state lasing at room temperature, featuring a critical temperature of 385 K for the 10-fold $In_{0.5}Ga_{0.5}As$ QD stack laser. The stacks were grown at the same low temperature for QD layers and

GaAs spacers. The performance has further been substantially improved by introducing temperature cycling to grow the spacer layers at increased temperature and to smoothen the spacer-QD interfaces [60]. QD layers represent small grouped peaks in the gain region, which is clad by the DBR and a window layer on the left- and right-hand sides, respectively. QD lasers benefit from the reduced lateral charge carrier diffusion due to trapping in the QDs [61–63]. The effect was shown to suppress beam filamentation observed in QW lasers [62]. Moreover, nonradiative surface recombination decreases. As a consequence, the robustness against facet degradation in high-power operation is enhanced, and deep etch through the active region in narrow-stripe ridges is possible without surface passivation [63]. Furthermore, using the Dot-in-a-Well (DWELL) approach through inserting a strain-reducing layer to reduce the strain exerted on the buried QD layer with respect to a cap and carefully adjusting the growth parameters for each individual QD layer in the stack to avoid defect formation, lasing at 1.25 μm with a very low threshold current density of 66 $A \cdot cm^{-2}$ and 94% internal quantum efficiency was obtained [64]. Besides, the target of lasing at 1.35 μm from ten stacked InAs-Sb:GaAs QD layers grown using MOVPE was accomplished with DWELL structure devices [65].

4 VECSELs based on QDs

4.1 Introduction to QD VECSELs

In this section, we focus on the properties and recent developments of semiconductor QD VECSELs based on two typical alternative paths for high-density QDs of gain layers. The unique properties of QDs inspired intensive studies to implement them into semiconductor VECSEL devices, as depicted in Fig. 2(b). QD VECSELs as a relatively recent type of semiconductor lasers are key building elements for optical communication systems. Historic trend predicts fourfold increase in the maximum commercial single channel data rate every five years [66]. At present, QD VECSELs span the 650 nm to 1.8 μm spectral range, with record *cw* output powers at room temperature [6,38,66]. QD VECSELs are usually optically pumped using diode lasers, with a cavity formed by an epitaxially grown gain mirror, consisting of an active region on top a DBR, and a second external mirror which also acts as an output coupler. The QD VECSEL allows the addition of intracavity elements including nonlinear crystals for frequency downconversion. These techniques have resulted in the use of near-IR VECSELs as frequency-doubled and quadrupled sources for visible and UV wavelengths. QDs have to be placed near the antinodes of this standing wave in order to provide efficient gain to the laser. This is the socalled resonant periodic gain (RPG) arrangement [6,13,42] of placing QD gain layer near a given standing wave antinode. In addition, QD VECSEL devices also demonstrate excellent dynamic performances such as low threshold currents (a few micro-amps), low noise operation and high-speed digital modulation (10 Gb/s) [66,67].

The crucial requirement of a high QD density in the volume of the gain medium can be realized by a high areal density and a dense stacking of QD layers technically, which is particularly challenging for QDs emitting at long wavelength because these QDs are comparably large and have consequently large strain fields. The design and growth procedure must avoid a strain-induced formation of defects, which may degrade the performance of the device. In addition, the strain-induced structural coupling of QDs in adjacent layers may lead to a vertical alignment with an increased inhomogeneous broadening due to a gradually increasing QD size [68]. Based on the thermal stability of covered dots below 600°C, a procedure to flatten the growth front prior to QD layer deposition and to overgrow the dots was established that maintains a high radiative recombination efficiency of the QDs [69]. One strategy that could be used to get to longer wavelengths would be to manage the strain through employing strain compensation; however, this technique has its limitations. The use of RPG structures with a single-QD layer per antinode is another way to control strain in such lasers. Since 2008, several first realized QD gain chips that implemented a layout of RPG structure to selectively enhance gain at the operating wavelength have further been reported [13,71–74].

Advances in growth control of high-quality QD layers eventually allowed the implementation of QDs also in gain media of semiconductor VECSELs [70–76]. Consequently, QDs for four working wavelengths of 940, 1040, 1180, and 1250 nm have been successfully implemented into the resonant gain structures of QD VECSEL devices. The Stranski–Krastanow and the submonolayer growth modes as two typical alternative paths for high-density QDs have been used for maximization of the gain region so far, and therefore the operation of VECSEL devices have been demonstrated with both the Stranski–Krastanow QDs [71,72,74] and submonolayer QDs [73,75,76]. Both kinds of QDs have quite different optical properties. The Stranski–Krastanow QDs show a very broad spectrum. On the other hand, the submonolayers QDs exhibit a narrow luminescence with a significant thermal shift. Careful adjustment of emission wavelength is therefore required. The first design intends to maximize the modal gain per dot layer, while the second design aims for a maximum total modal gain by increasing the number of QD layers.

4.2 VECSELs with Stranski-Krastanow QDs

The first implementation of Stranski–Krastanow QDs employed in semiconductor QD VECSELs for 1040 nm emission [71], in which the QD layers were integrated into

a resonant gain structure. Surface photoluminescence (PL) occurs at the wavelength of the small dip in the reflectivity of the DBR stopband that is attributed to the subcavity resonance. The lasing spectrum of the Stranski-Krastanow QD VECSEL device in Ref. [71] shows Fabry-Perot fringes due to the etalon effect of the diamond intra cavity heat spreader. The threshold pump power is 6.5 W and the slope efficiency is 6.7%. At high pump power, an onset of thermal rollover occurs. As we have mentioned before, one potential benefit of employing QDs instead of QWs in a gain medium is the achievement of a low lasing threshold with much smaller temperature dependence. Moreover, by way of elastic strain relaxation in a uniform arrangement of 7×3 Stranski-Krastanow grown QD layers, GaAs QD laser devices for 1220 nm operation have been achieved to extend the operation wavelength to the near-IR range [72]. The device showed a threshold pump power of 0.48 W at 15°C for a high reflectivity (99.8%) output coupler mirror. Notably, the results demonstrate temperature-stable operation in the measured range. The dependence on pump power density is only $0.027\,\mathrm{nm}\cdot(\mathrm{kW}\cdot\mathrm{cm}^{-2})^{-1}$. The center wavelength of the emission shifts only by $0.06\,\mathrm{nm}\cdot\mathrm{K}^{-1}$, leaving the output power largely unaffected. Such shift is almost an order of magnitude smaller than typical values of $0.3\,\mathrm{nm}\cdot\mathrm{K}^{-1}$ observed for VECSELs based on GaInNAs QWs [67], and the temperature-independent differential efficiency of the device is about 2%. The use of InAs QD active regions for VECSELs could achieve high-power lasers in the 900–1300 nm wavelength range.

Very recently, Albrecht et al. [13] have demonstrated the growth of 1250 nm emission wavelength InAs-QD VECSELs and achieved better lasing performance by designing two different RPG structures with increased spacing between the QD layers, thus allowing the crystal to recover between each QD layer growth. The first laser is based on the traditional multi-QD layer per antinode design, which is referred to as the "4×3" structure (four sets of three QD layers). The second laser that utilize a single-QD layer per antinode with "12×1" structure has demonstrated 3.25 W of *cw* output power using a chemical vapor deposition (CVD) diamond heat spreader mounted to the thinned substrate of the "12×1" structure. The active region growth for the two VECSELs is based on identical QD structures, and the emission wavelength for the two structures is around 1250 nm. For both designs, highly optimized QD structures for maximum gain are made through the use of DWELL structures. The QDs are designed for 1250 nm emission and are grown with a total thickness of 1.68 monolayers of InAs deposited after growing 1 nm of 7 nm total thickness $In_{0.15}Ga_{0.85}As$ QW. The only variation in the two VECSELs is the design of the RPG active region and the active RPG region is grown at a substrate temperature of 480°C. The increased separation between the dot layer in the "12×1" structure compared to the "4×3" structure resulted in superior lasing performance with regard to the threshold pump-power density, the slope efficiency, and the maximum output power. An important issue for the further development of QD VECSELs is the dense stacking of QD layers.

4.3 VECSELs with submonolayer QDs

As a practical alternative approach, the submonolayer QDs were implemented in semiconductor QD disk lasers for 940 nm [75] and 1040 nm emission [73]. The submonolayer QDs were grown by cycled depositions of pure binaries InAs and GaAs. The tuning of the emission wavelength may be performed by adjusting either the InAs deposition duration or the number of InAs/GaAs cycles. As a matter of fact, the wavelength control is somewhat facilitated by adjusting the number of cycles, yielding robust reproducibility with similar optical performance. The wavelength tuning of submonolayer QDs must consider proper alignment of the PL peak wavelength with the cavity resonance of the VECSEL structure. The submonolayer QDs for the emission wavelength of 940 nm were grown using a fivefold cycle of 0.5 monolayer InAs and 2.3 monolayer GaAs. Studies of stacking three such submonolayer QD layers using GaAs spacers from 60 to 10 nm showed a constant high PL intensity down to 20 nm thickness and a drop of intensity for thinner spacers. A thickness of 20 nm for three layers in an antinode was therefore chosen for device applications to obtain a large overlap to the optical field in the gain region.

Submonolayer QDs for 1040 nm operation were grown in the same way with 10 InAs/GaAs cycles of nominally 0.5 monolayer InAs and 2.3 monolayer GaAs as those for 940 nm emission [73]. A minimum spacer thickness of 20 nm could be achieved without structural degradation. Wavelength tuning was performed by increasing the number of submonolayer cycles per submonolayer-QD layer. Limits for the given conditions were found to be 1070 and 960 nm for the long and short wavelength side, respectively. Results on QD VECSELs achieved thus far yield a higher gain achieved with submonolayer QDs, accompanied by a smaller wavelength range of gain. For the case of 1035 nm wavelength emission, 13 submonolayer-QD layers, each comprising 10-fold cycled depositions of nominally 0.5 monolayer InAs and 2.3 monolayer GaAs, were integrated into a gain structure [67]. Compared to Stranski–Krastanow QDs, the larger gain of submonolayer-QDs leads to increased slope efficiency. Characteristics of the device yield a slope efficiency of up to 12.4%. Due to a larger efficiency, no significant thermal rollover is observed. A maximum *cw* output power of 1.4 W is obtained for 1% outcoupling. Good characteristics were likewise obtained from a submonolayer-QD VECSEL fabricated for 940 nm emission [75]. An output power of 0.5 W at 1% outcoupling was achieved using 10 layers of fivefold cycled submonolayer-QDs. Notably, the low value originates from the limited modal gain of the structure and is an issue of future improvements.

5 Ultimate nanolasers: single QD VECSEL devices

In this part, we discuss the development and current status of a single-QD-cavity coupled system. Over the past ten years, the possibility of realizing a single QD nanolaser (the socalled thresholdless laser) in which the threshold is ultimately eliminating has been drawing intensive attention. As an ultimate microscopic limit of thresholdless semiconductor lasers, single-QD nanolaser, i.e., a single QD coupled to a single mode of an optical cavity shown in Fig. 4, allow us to investigate the light–matter interaction down to the single particle level entering the so-called cavity QED regime [4,77,78]. As early as in 1999, Pelton and Yamamoto [77] firstly proposed a single QD microcavity system as a novel ultralow threshold laser device, consisting of a single InAs/GaAs self-assembled QD coupled to a highfinesse microsphere cavity. Later, Strauf and Jahnke have demonstrated that very few (2–4) QDs as a gain medium are sufficient to realize a photonic crystal (PhC) laser based on a high-quality nanocavity [78]. Photon correlation measurements show a transition from a thermal to a coherent light state proving that lasing action occurs at ultralow thresholds. They conclude that the quasicontinuous QD states become crucial since they provide an energy transfer channel into the lasing mode, effectively leading to a self-tuned resonance for the gain medium. In 2006, for applications in low THz sources (1 THz) for molecular detection in chemistry and biology as well as THz-band communications between 0.8–3 THz, we proposed and examined a terahertz laser model based on a single InAs semiconductor QD emitter in a microcavity [39], in which single InAs QD is selectively placed in a high quality microdisk cavity, as shown in Figs. 4(a) and 4(b), which is resonant with an intersublevel transition (ISBT) between quasicontinuous states of QD. Specifically, to achieve the desired long-wavelength of THz, an intersublevel lasing transition is from an excited conduction band state to a lower conduction band state between quasicontinuous states of the InAs QD emitters. The microdisk cavity is tuned to the radiative transition resonance, so likely the final transition emptying this state will be off resonance [39]. An increase in DOS of the lasing mode causes significant enhancement of the spontaneous emission rate (Purcell effect) [77]. This consequently enables larger fractions of photons to be emitted into the lasing mode with respect to all other modes (denoted as spontaneous emission-coupling factor β) and reduces the lasing threshold [39,77–83]. Here we want to point out that from the viewpoint of photonic quantum information processing, such a single-QD-microcavity system can also be well-suited for single-photon generation [1,4,78–80].

Furthermore, PhC nanocavities [81,84–89] are also promising candidates for the trapping of light in ultrasmall volumes with high Q – factor. And a QD with 3D carrier

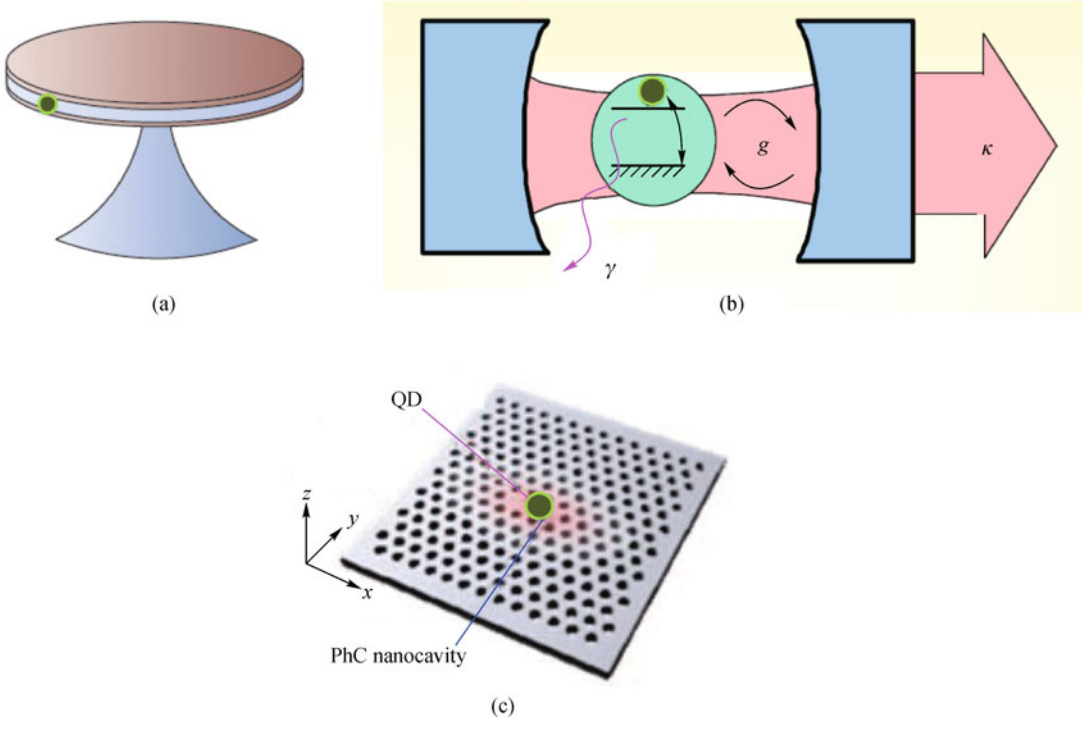

Fig. 4 Schematic structure (a) and corresponding working mechanism (b) of single QD microdisk nanolaser, in which an atomic QD in a small-volume microdisk cavity with dephasing rate γ coupled to a cavity with photon loss rate κ by coupling strength g. (c) Schematic illustration of the QD-PhC-nanocavity system considered, in which a single QD embedded in a PhC nanocavity

confinement as the most suitable gain medium can be introduced into a PhC nanocavity, avoiding the effects of nonradiative centers that are inevitably introduced in the fabrication of PhCs and thereby restricting the coupling of the QD gain medium to the lasing mode. Recently, such a coupled system consisting of a nanocavity and a QD shown in Fig. 4(c) has been further extensively investigated because of its promising applications such as quantum information processing [4,83–86], single photon sources [1,81,85], and ultimately low-threshold nanolasers [78,80,86–89]. For such a single QD PhC nanocavity system, utilization of a single mode cavity with a sufficiently high Q factor as a lasing mode, the modal volume of which should be as small as possible to maximize the interaction with the single QD gain medium, is key to realize a thresholdless QD nanolaser. For such a single-QD-nanocavity system the two phenomena that light should be emitted only at the QD transition energy under off-resonant conditions and vacuum Rabi splitting (VRS) should occur under on-resonant conditions are expected to occur naturally, analogous to the atomic systems in cavity QED [89]. However, experimental reports have shown clear deviations from these features. First, light emission from the cavity occurs even when it is largely detuned from the QD [83,84,86,87]. Second, spectral triplets are formed by additional bare cavity lines between the VRS lines under on-resonant conditions [86,87]. These features are unique to semiconductor nanostructure systems and are not predicted by conventional cavity QED in atomic systems. In our study, the QD was typically modeled by a simple atomic two-level system and the effect of pure dephasing was to broaden the transition energy of the two-level system [39,86], which makes it possible for the tail of the transition energy to overlap with the cavity energy, and generates an additional way in which to interact with the cavity. Owing to this interaction, a cavity photon is created with the transition of the excited two-level system to the ground state, a process generally known as the anti-Zeno effect (AZE), induced by pure dephasing in the QD. In most cases, this effect could be negligible, because the tail of the atomic two-level system transition energy at the cavity energy is so weak that the interaction is not large enough to overcome the direct spontaneous emission from the two-level system to free space. However, the unique situation achieved in nanocavity QED systems strongly enhances the AZE, resulting in off-resonant cavity light emission due to the following reasons. First, the coupling constant between the cavity and the two-level system is large due to the small cavity volume. Second, the quality factor of the cavity is relatively large. Third, direct spontaneous emission from the two-level system to free space is strongly suppressed due to the in-plane photonic band-gap effect in the case of the 2D PhC nanocavities shown in Fig. 4(c) [84–86]. These features are well described by a factor F, which is given by

$$F \approx \frac{\Gamma_{\text{spon}} + \gamma_{\text{phase}}}{\Gamma_{\text{spon}}(\delta\omega_{\text{TLS,c}}/g_{\text{TLS,c}})^2 + \Gamma_{\text{c}} + (\Gamma_{\text{spon}} + \gamma_{\text{phase}})}, \quad (2)$$

where Γ_{spon} is the direct spontaneous emission rate of the TLS to free space, Γ_{c} is the damping rate of the cavity, which is determined by its Q factor, γ_{phase} is the pure dephasing rate of the TLS, $\delta\,\omega_{\text{TLS,c}}$ is the detuning of the TLS from the cavity, and $g_{\text{TLS,c}}$ is the coupling constant between the TLS and the cavity. Thus, the off-resonant cavity light emission can successfully be explained by this nanocavity-enhanced AZE, and we conclude that the phenomenon of most low-dimensional semiconductor nanostructures in PhC nanocavities cannot be fully describes by atomic two-level systems in cavity QED. Furthermore, by comparing the intensity of the central peak in the triplet with the values predicted by the factor F, we conclude that the on-resonant triplet is explained well by the AZE from the detuned states under a low-excitation regime. A similar analysis was also reported independently by Yamaguchi et al. [85]. Their calculated results reproduce the features of the experimentally observed on-resonant spectral triplet, the origin of which has puzzled the community for several years. Such a formalism should prove to be useful for future studies, such as practical analyses of quantum information processing using QD spins and cavity QED [4,80,85–87], as well as studies of the design and optimization of the performance of single photon sources [1,82,85]. We believe that these results above will stimulate a full understanding of the physical nature of solid-state cavity QED systems. A pulsed QD nanocavity could serve as a single photon turnstile that is more deterministic than one based on Purcell enhancement [77,78,80]. Controlled quantum entanglement in a QD nanocavity could be used for quantum state transfer where true strong-coupling serves as a bidirectional interface between semiconductor and photonic quantum states, as required in a quantum information network [1,90]. In the future, large-scale monolithic photonic integrated circuits (MPhICs) represent a significant technology innovation that simplifies optical communication system design, reduces space and power consumption, and improves reliability. In addition, by lowering the cost of optical-to-electrical-to-optical (OEO) conversion in optical networks, QD nanolaser provides a transformational opportunity to embrace the use of monolithic electronic silicon ICs and system software in a “digital” optical network to maximize system functionality, improve service flexibility, and simplify network operations.

6 Conclusions

This review has discussed properties and advantages of semiconductor VECSELs, and properties and recent development of QD lasers, as a building block for practical

optical communication systems. In particular, this review outlines the properties and recent proofs of developments of QD VECSEL devices in detail. In the final section of this review, from the viewpoint of both the single QD nanolaser device and cavity QED, we present the theory, model and analysis of a coupled system consisting of a nanocavity and a QD. Although recent pioneering developments in nanofabrication technologies are beginning to realize such systems, precise tuning between the single QD and PhC nanocavity, which is critical to the realization of a single QD nanolaser and single-photon source needs to be further improved in future. The presented results in this review are important for the future development of QD VECSEL technology or even MPhICs and quantum information devices.

Acknowledgements The research conducted in State Key Laboratory of Functional Material for Informatics has been supported by the Major State Basic Research Development Program of China (No. 2009CB930600), and by a Strategic Research Grant (No. 7008101) from City University of Hong Kong.

References

1. Michler P, Kiraz A, Becher C, Schoenfeld W V, Petroff P M, Zhang L, Hu E, Imamoglu A. A quantum dot single-photon turnstile device. Science, 2000, 290(5500): 2282–2285
2. Fonoberov V A, Balandin A A. ZnO quantum dots: physical properties and optoelectronic applications. Journal of Nanoelectronics and Optoelectronics, 2006, 1(1): 19–38
3. Kumano H, Kimura S, Endo M, Sasakura H, Adachi S, Muto S, Suemune I. Deterministic single-photon and polarization-correlated photon pair generations from a single InAlAs quantum dot. Journal of Nanoelectronics and Optoelectronics, 2006, 1(1): 39–51
4. Gerard J M, Gayral B. InAs quantum dots: artificial atoms for solid-state cavity-quantum electrodynamics. Physica E, Low-Dimensional Systems and Nanostructures, 2001, 9(1): 131–139
5. Fathpour S, Mi Z, Bhattacharya P. High-speed quantum dot lasers. Journal of Physics D, 2005, 38(13): 2103–2111
6. Okhotnikov O G. Seminconductor Disk Laser. Berlin: Wiley-VCH Verlag, 2010
7. Vallaitis T, Koos C, Bonk R, Freude W, Laemmlin M, Meuer C, Bimberg D, Leuthold J. Slow and fast dynamics of gain and phase in a quantum dot semiconductor optical amplifier. Optics Express, 2008, 16(1): 170–178
8. Murray C B, Norris D J, Bawendi M G. Synthesis and characterization of nearly monodisperse CdE (E = sulfur, selenium, tellurium) semiconductor nanocrystallites. Journal of the American Chemical Society, 1993, 115(19): 8706–8715
9. He Y, Lu H T, Sai L M, Lai W Y, Fan Q L, Wang L H, Huang W. Synthesis of CdTe nanocrystals through program process of microwave irradiation. Journal of Physical Chemistry B, 2006, 110(27): 13352–13356
10. Shan G, Bao S, Shek C H, Huang W. Theoretical study of fluorescence resonant energy transfer dynamics in individual semiconductor nanocrystal-DNA-dye conjugates. Journal of Luminescence, 2012, 132(6): 1472–1476
11. Kuznetsov M, Hakimi F, Sprague R, Mooradian A. Design and characteristics of high-power (> 0.5-W CW) diode-pumped vertical-external-cavity surface-emitting semiconductor lasers with circular TEM_{00} beams. IEEE Journal on Selected Topics in Quantum Electronics, 1999, 5(3): 561–573
12. Rantamäki A, Sirbu A, Mereuta A, Kapon E, Okhotnikov O G. 3 W of 650 nm red emission by frequency doubling of wafer-fused semiconductor disk laser. Optics Express, 2010, 18(21): 21645–21650
13. Albrecht A R, Hains C P, Rotter T J, Stintz A, Malloy K J, Balakrishnan G, Moloney J V. High power 1.25 μm InAs quantum dot vertical external-cavity surface-emitting laser. Journal of Vacuum Science & Technology B, 2011, 9(3): 03C113
14. Coldren L A, Corzine S W. Diode Lasers and Photonic Integrated Circuits. New York: John Wiley & Sons, 1995
15. Li H, Iga K. Vertical-Cavity Surface-Emitting Laser Devices. Berlin: Springer, 2002
16. Diehl R. High Power Diode Lasers. Berlin: Springer, 2000
17. Lutgen S, Albrecht T, Brick P, Reill W, Luft J, Späth W. 8-W high-efficiency continuous-wave semiconductor disk laser at 1000 nm. Applied Physics Letters, 2003, 82(21): 3620
18. Kapon E. Semiconductor Lasers II: Materials and Structures. New York: Academic Press, 1999
19. Chilla J, Shu Q Z, Zhou H, Weiss E, Reed M, Spinelli L. Recent advances in optically pumped semiconductor lasers. In: Proceedings of the Society for Photo-Instrumentation Engineers, 2007, 6451: 645109
20. Keller U, Tropper A C. Passively modelocked surface-emitting semiconductor lasers. Physics Reports, 2006, 429(2): 67–120
21. Saarinen E J, Härkönen A, Suomalainen S, Okhotnikov O G. Power scalable semiconductor disk laser using multiple gain cavity. Optics Express, 2006, 14(26): 12868–12871
22. Fan L, Fallahi M, Hader J, Zakharian A R, Moloney J V, Murray J T, Bedford R, Stolz W, Koch S W. Multichip vertical-external-cavity surface-emitting lasers: a coherent power scaling scheme. Optics Letters, 2006, 31(24): 3612–3614
23. Fan L, Fallahi M, Zakharian A, Hader J, Moloney J V, Bedford R, Murray J T, Stolz W, Koch S W. Extended tunability in a two-chip VECSEL. IEEE Photonics Technology Letters, 2007, 19(8): 544–546
24. Rautiainen J, Härkönen A, Korpijärvi V M, Tuomisto P, Guina M, Okhotnikov O G. 2.7 W tunable orange-red GaInNAs semiconductor disk laser. Optics Express, 2007, 15(26): 18345–18350
25. Hilbich S, Seelert W, Ostroumov V, Kannengiesser C, Elm R v, Mueller J, Weiss E, Zhou H, Chilla J. New wavelengths in the yellow orange range between 545 nm and 580 nm generated by an intracavity frequency-doubled optically pumped semiconductor laser. Proceedings of SPIE, 2007, 6451: 64510C
26. Fallahi M, Fan L, Kaneda Y, Hessenius C, Hader J, Li H, Moloney J V, Kunert B, Stolz W, Koch S W, Murray J, Bedford R. 5-W yellow laser by intracavity frequency doubling of high-power vertical-external-cavity surface-emitting laser. IEEE Photonics Technology Letters, 2008, 20(20): 1700–1702
27. Giet S, Sun H D, Calvez S, Dawson M D, Suomalainen S, Harkonen A, Guina M, Okhotnikov O, Pesa M. Spectral narrowing and

locking of a vertical-external-cavity surface-emitting laser using an intracavity volume Bragg grating. IEEE Photonics Technology Letters, 2006, 18(16): 1786–1788

28. Giet S, Lee C L, Calvez S, Dawson M D, Destouches N, Pommier J C, Parriaux O. Stabilization of a semiconductor disk laser using an intra-cavity high reflectivity grating. Optics Express, 2007, 15(25): 16520–16526
29. Fan L, Fallahi M, Murray J T, Bedford R, Kaneda Y, Zakharian A R, Hader J, Moloney J V, Stolz W, Koch S W. Tunable high-power high-brightness linearly polarized vertical-external-cavity surface-emitting lasers. Applied Physics Letters, 2006, 88(2): 021105
30. Lorenser D, Maas D, Unold H J, Bellancourt A R, Rudin B, Gini E, Ebling D, Keller U. 50-GHz passively mode-locked surface-emitting semiconductor laser with 100-mW average output power. IEEE Journal of Quantum Electronics, 2006, 42(8): 838–847
31. Haring R, Paschotta R, Aschwanden A, Gini E, Morier-Genoud F, Keller U. High-power passively mode-locked semiconductor lasers. IEEE Journal of Quantum Electronics, 2002, 38(9): 1268–1275
32. Alford W J, Raymond T D, Allerman A A. High power and good beam quality at 980 nm from a vertical external-cavity surface-emitting laser. Journal of the Optical Society of America B: Optical Physics, 2002, 19(4): 663–666
33. Hastie J E, Hopkins J M, Calvez S, Jeon C W, Burns D, Abram R, Riis E, Ferguson A I, Dawson M D. 0.5-W single transverse-mode operation of an 850-nm diode-pumped surface-emitting semiconductor laser. IEEE Photonics Technology Letters, 2003, 15(7): 894–896
34. Hastie J E, Morton L G, Calvez S, Dawson M D, Leinonen T, Pessa M, Gibson G, Padgett M J. Red microchip VECSEL array. Optics Express, 2005, 13(18): 7209–7214
35. Kemp A J, Maclean A J, Hastie J E, Smith S A, Hopkins J M, Calvez S, Valentine G J, Dawson M D, Burns D. Thermal lensing, thermal management and transverse mode control in microchip VECSELs. Applied Physics B: Lasers and Optics, 2006, 83(2): 189–194
36. Garnache A, Kachanov A A, Stoeckel F, Planel R. High-sensitivity intracavity laser absorption spectroscopy with vertical-external-cavity surface-emitting semiconductor lasers. Optics Letters, 1999, 24(12): 826–828
37. Zhao X H, Zhao X, Shan G C, Gao Y. Fiber-coupled laser-driven flyer plates system. Review of Scientific Instruments, 2011, 82(4): 043904
38. Dingle R, Henry C H. Quantum effects in heterostructure lasers. US Patent, 3 982 207, 1976
39. Shan G C, Bao S Y. Theoretical study of a quantum dot microcavity laser. Proceedings of the SPIE, 2007, 6279: 627925
40. Bimberg D, Kirstaedter N, Ledentsov N N, Alferov Zh I, Kopev P S, Ustinov V M. InGaAs-GaAs quantum-dot lasers. IEEE Journal on Selected Topics in Quantum Electronics, 1997, 3(2): 196–205
41. Asada M, Miyamoto Y, Suematsu Y. Gain and the threshold of three-dimensional quantum-box lasers. IEEE Journal of Quantum Electronics, 1986, QE-22(9): 1915–1921
42. Kirstaedter N, Schmidt O G, Ledentsov N N, Bimberg D, Ustinov V M, Egorov A Yu, Zhukov A E, Maximov M V, Kopev P S, Alferov Zh I. Gain and differential gain of single layer InAs/GaAs quantum dot injection lasers. Applied Physics Letters, 1996, 69(9): 1226
43. Jiang H, Singh J. Nonequilibrium distribution in quantum dots lasers and influence on laser spectral output. Journal of Applied Physics, 1999, 85(10): 7438
44. Leonard D, Pond K, Petroff P M. Critical layer thickness for self-assembled InAs islands on GaAs. Physical Review B: Condensed Matter and Materials Physics, 1994, 50(16): 11687–11692
45. Bester G, Wu X, Vanderbilt D, Zunger A. Importance of second-order piezoelectric effects in zinc-blende semiconductors. Physical Review Letters, 2006, 96(18): 187602
46. Schliwa A, Winkelnkemper M, Bimberg D. Impact of size, shape, and composition on piezoelectric effects and electronic properties of In(Ga)As/GaAs quantum dots. Physical Review B: Condensed Matter and Materials Physics, 2007, 76(20): 205324
47. Schliwa A, Winkelnkemper M, Bimberg D. Few-particle energies versus geometry and composition of $In_xGa_{1-x}As/GaAs$ self-organized quantum dots. Physical Review B: Condensed Matter and Materials Physics, 2009, 79(7): 075443
48. Vallaitis T, Koos C, Bonk R, Freude W, Laemmlin M, Meuer C, Bimberg D, Leuthold J. Slow and fast dynamics of gain and phase in a quantum dot semiconductor optical amplifier. Optics Express, 2008, 16(1): 170–178
49. Blokhin S A, Maleev N A, Kuzmenkov A G, Sakharov A V, Kulagina M M, Shernyakov Yu M, Novikov I I, Maximov M V, Ustinov V M, Kovsh A R, Mikhrin S S, Ledentsov N N, Lin G, Chi J Y. Vertical-cavity surface-emitting lasers based on submonolayer InGaAs quantum dots. IEEE Journal of Quantum Electronics, 2006, 42(9): 851–858
50. Mutig A, Fiol G, Moser P, Arsenijevic D, Shchukin V A, Ledentsov N N, Mikhrin S S, Krestnikov I L, Livshits D L, Kovsh A R, Hopfer F, Bimberg D. 120°C 20 Gbit/s operation of 980 nm VCSEL. Electronics Letters, 2008, 44(22): 1305–1306
51. Sellin R L, Kaiander I, Ouyang D, Kettler T, Pohl U W, Bimberg D, Zakharov N D, Werner P. Alternative-precursor metalorganic chemical vapor deposition of self-organized InGaAs/GaAs quantum dots and quantum-dot lasers. Applied Physics Letters, 2003, 82(6): 841
52. Sellers I R, Liu H Y, Groom K M, Childs D T, Robbins D, Badcock T J, Hopkinson M, Mowbray D J, Skolnick M S. 1.3 μm InAs/GaAs multilayer quantum-dot laser with extremely low room-temperature threshold current density. Electronics Letters, 2004, 40(22): 1412–1413
53. Xu Z, Birkedal D, Juhl M, Hvam J. Submonolayer InGaAs/GaAs quantum-dot lasers with high modal gain and zero-linewidth enhancement factor. Applied Physics Letters, 2004, 85 (15): 3259
54. Mikhrin S S, Zhukov A E, Kovsh A R, Maleev N A, Ustinov V M, Shernyakov Yu M, Soshnikov I P, Livshits D L, Tarasov I S, Bedarev D A, Volovik B V, Maximov V M, Tsatsulnikov A F, Ledentsov N N, Kopev P S, Bimberg D, Alferov Zh I. 0.94 μm diode lasers based on Stranski-Krastanow and sub-monolayer quantum dots. Semiconductor Science and Technology, 2000, 15 (11): 1061–1064
55. Vahala K J. Quantum box fabrication tolerance and size limits in semiconductors and their effect on optical gain. IEEE Journal of Quantum Electronics, 1988, 24(3): 523–530
56. Kirstaedter N, Ledentsov N N, Grundmann M, Bimberg D, Ustinov

V M, Ruvimov S S, Maximov M V, Kopev P S, Alferov Zh I, Richter U, Werner P, Gosele U, Heydenreich J. Low threshold, large T_0 injection laser emission from (InGa)As quantum dots. Electronics Letters, 1994, 30(17): 1416–1417

57. Marko I P, Andreev A D, Adams A R, Krebs R, Reithmeier J, Forchel A. Importance of Auger recombination in InAs 1.3 μm quantum dot lasers. Electronics Letters, 2003, 39(1): 58
58. Shchekin O B, Deppe D G. Low-threshold high-T_0/1.3-μm InAs quantum-dot lasers due to p-type modulation doping of the active region. IEEE Photonics Technology Letters, 2002, 14(9): 1231–1233
59. Heinrichsdorff F, Mao M H, Kirstaedter N, Krost A, Bimberg D, Kosogov A O, Werner P. Room-temperature continuous-wave lasing from stacked InAs/GaAs quantum dots grown by metalorganic chemical vapor deposition. Applied Physics Letters, 1997, 71 (1): 22
60. Maximov M V, Kochnev I V, Shernyakov Y M, Zaitsev S V, Gordeev N Yu, Tsatsulnikov A F, Sakharov A V, Krestnikov I L, Kopev P S, Alferov Zh I, Ledentsov N N, Bimberg D, Kosogov A O, Werner P, Gösele U. InGaAs/GaAs quantum dot lasers with ultrahigh characteristic temperature (T_0 = 385 K) grown by metal organic chemical vapour deposition. Japanese Journal of Applied Physics, 1997, 36(Part 1, No. 6B): 4221–4223
61. Sellin R L, Heinrichsdorff F, Ribbat Ch, Grundmann M, Pohl U W, Bimberg D. Surface flattening during MOCVD of thin GaAs layers covering InGaAs quantum dots. Journal of Crystal Growth, 2000, 221(1–4): 581–585
62. Ribbat Ch, Sellin R L, Kaiander I, Hopfer F, Ledentsov N N, Bimberg D, Kovsh A R, Ustinov V M, Zhukov A E, Maximov M V. Complete suppression of filamentation and superior beam quality in quantum-dot lasers. Applied Physics Letters, 2003, 82(6): 952
63. Ouyang D, Ledentsov N N, Bognar S, Hopfer F, Sellin R L, Kaiander I, Bimberg D. Impact of the mesa etching profiles on the spectral hole burning effects in quantum dot lasers. Semiconductor Science and Technology, 2004, 19(5): L43–L47
64. Strittmatter A, Germann T D, Kettler Th, Posilovic K, Pohl U W, Bimberg D. Alternative precursor metal-organic chemical vapor deposition of InGaAs/GaAs quantum dot laser diodes with ultralow threshold at 1.25 μm. Applied Physics Letters, 2006, 88(26): 262104
65. Guimard D, Ishida M, Hatori N, Nakata Y, Sudo H, Yamamoto T, Sugawara M, Arakawa Y. CW lasing at 1.35 μm from ten InAs–Sb: GaAs quantum-dot layers grown by metal-organic chemical vapor deposition. IEEE Photonics Technology Letters, 2008, 20(10): 827–829
66. Kaminow I, Li T Y, Willner A. Optical Fiber Telecommunications V A. 5th ed. Components and Subsystems, Elsevier, 2008
67. Konttinen J, Harkonen A, Tuomisto P, Guina M, Rautiainen J, Pessa M, Okhotnikov O. High-power (> 1 W) dilute nitride semiconductor disk laser emitting at 1240 nm. New Journal of Physics, 2007, 9 (5): 140
68. Lita B, Goldman R S, Philips J D, Bhattacharya P K. Nanometer-scale studies of vertical organization and evolution of stacked self-assembled InAs/GaAs quantum dots. Applied Physics Letters, 1999, 74(19): 2824
69. Heinrichsdorff F, Grundmann M, Stier O, Krost A, Bimberg D. Influence of In/Ga intermixing on the optical properties of InGaAs/GaAs quantum dots. Journal of Crystal Growth, 1998, 195(1–4): 540–545
70. Lagatsy A A, Bain F M, Brown C T A, Sibbett W, Livshits D A, Erbert G, Rafailov E U. Low-loss quantum-dot-based saturable absorber for efficient femtosecond pulse generation. Applied Physics Letters, 2007, 91: 231111
71. Strittmatter A, Germann T D, Pohl J, Pohl U W, Bimberg D, Rautiainen J, Guina M, Okhotnikov O G. 1040 nm vertical external cavity surface emitting laser based on InGaAs quantum dots grown in Stranski-Krastanow regime. Electronics Letters, 2008, 44(4): 290–291
72. Germann T D, Strittmatter A, Pohl J, Pohl U W, Bimberg D, Rautiainen J, Guina M, Okhotnikov O G. Temperature-stable operation of a quantum dot semiconductor disk laser. Applied Physics Letters, 2008, 93(5): 051104
73. Germann T D, Strittmatter A, Pohl J, Pohl U W, Bimberg D, Rautiainen J, Guina M, Okhotnikov O G. High-power semiconductor disk laser based on InAs/GaAs submonolayer quantum dots. Applied Physics Letters, 2008, 92(10): 101123
74. Lenz A, Eisele H, Timm R, Hennig Ch, Becker S K, Sellin R L, Pohl U W, Bimberg D, Dahne M. Nanovoids in InGaAs/GaAs quantum dots observed by cross-sectional scanning tunneling microscopy. Applied Physics Letters, 2004, 85(17): 3848
75. Germann T D, Strittmatter A, Pohl U W, Bimberg D, Rautiainen J, Guina M, Okhotnikov O G. Quantum-dot semiconductor disk lasers. Journal of Crystal Growth, 2008, 310(23): 5182–5186
76. Germann T D, Strittmatter A, Kettler T, Posilovic K, Pohl U W, Bimberg D. MOCVD of InGaAs/GaAs quantum dots for lasers emitting close to 1.3 μm. Journal of Crystal Growth, 2007, 298: 591–594
77. Pelton M, Yamamoto Y. Ultralow threshold laser using a single quantum dot and a microsphere cavity. Physical Review A, 1999, 59 (3): 2418–2421
78. Strauf S, Jahnke F. Single quantum dot nanolaser. Laser Photonics Reviews, 2011, 5(5): 607–633
79. Strauf S, Hennessy K, Rakher M T, Choi Y S, Badolato A, Andreani L C, Hu E L, Petroff P M, Bouwmeester D. Self-tuned quantum dot gain in photonic crystal lasers. Physical Review Letters, 2006, 96 (12): 127404
80. Pelton M, Santori C, Vucković J, Zhang B, Solomon G S, Plant J, Yamamoto Y. Efficient source of single photons: a single quantum dot in a micropost microcavity. Physical Review Letters, 2002, 89 (23): 233602
81. Song B S, Noda S, Asano T, Akahane Y. Ultra-high-Q photonic double-heterostructure nanocavity. Nature Materials, 2004, 4(3): 207–210
82. Lodahl P, Floris Van Driel A, Nikolaev I S, Irman A, Overgaag K, Vanmaekelbergh D, Vos W L. Controlling the dynamics of spontaneous emission from quantum dots by photonic crystals. Nature, 2004, 430(7000): 654–657
83. Reithmaier J P, Sek G, Löffler A, Hofmann C, Kuhn S, Reitzenstein S, Keldysh L V, Kulakovskii V D, Reinecke T L, Forchel A. Strong coupling in a single quantum dot-semiconductor microcavity system. Nature, 2004, 432(7014): 197–200
84. Yoshie T, Scherer A, Hendrickson J, Khitrova G, Gibbs H M,

Rupper G, Ell C, Shchekin O B, Deppe D G. Vacuum Rabi splitting with a single quantum dot in a photonic crystal nanocavity. Nature, 2004, 432(7014): 200–203

85. Yamaguchi M, Asano T, Noda S. Photon emission by nanocavity-enhanced quantum anti-Zeno effect in solid-state cavity quantum-electrodynamics. Optics Express, 2008, 16(22): 18067–18081
86. Yao P J, Rao M V S C, Hughes S. On-chip single photon sources using planar photonic crystals and single quantum dots. Laser & Photonics Reviews, 2010, 4(4): 499–516
87. Hennessy K, Badolato A, Winger M, Gerace D, Atatüre M, Gulde S, Fält S, Hu E L, Imamoğlu A. Quantum nature of a strongly coupled single quantum dot-cavity system. Nature, 2007, 445(7130): 896–899
88. Shan G C, Zhao X H, Huang W. Nanolaser with a single-graphene-nanoribbon in a microcavity. Journal of Nanoelectronics and Optoelectronics, 2011, 6(2): 138–143
89. Nomura M, Kumagai N, Iwamoto S, Ota Y, Arakawa Y. Laser oscillation in a strongly coupled single-quantum-dot-nanocavity system. Nature Physics, 2010, 6(4): 279–283
90. Cirac J I, Zoller P, Kimble H J, Mabuchi H. Quantum State Transfer and Entanglement Distribution among Distant Nodes in a Quantum Network. Physical Review Letters, 1997, 78(16): 3221–3224